

## Statistical description of tropospheric delay for InSAR : Overview and a new model

**Merryman Boncori, John Peter; Mohr, Johan Jacob**

*Published in:*

IEEE International Geoscience and Remote Sensing Symposium '07

*Link to article, DOI:*

[10.1109/IGARSS.2007.4423851](https://doi.org/10.1109/IGARSS.2007.4423851)

*Publication date:*

2007

*Document Version*

Publisher's PDF, also known as Version of record

[Link back to DTU Orbit](#)

*Citation (APA):*

Merryman Boncori, J. P., & Mohr, J. J. (2007). Statistical description of tropospheric delay for InSAR : Overview and a new model. In IEEE International Geoscience and Remote Sensing Symposium '07: IGARSS '07 (pp. 4483-4486). IEEE. DOI: 10.1109/IGARSS.2007.4423851

## DTU Library

Technical Information Center of Denmark

---

### General rights

Copyright and moral rights for the publications made accessible in the public portal are retained by the authors and/or other copyright owners and it is a condition of accessing publications that users recognise and abide by the legal requirements associated with these rights.

- Users may download and print one copy of any publication from the public portal for the purpose of private study or research.
- You may not further distribute the material or use it for any profit-making activity or commercial gain
- You may freely distribute the URL identifying the publication in the public portal

If you believe that this document breaches copyright please contact us providing details, and we will remove access to the work immediately and investigate your claim.

# Statistical Description of Tropospheric Delay for InSAR: Overview and a New Model

J.P. Merryman Boncori, J.J. Mohr  
 Technical University of Denmark  
 Ørsted-DTU  
 Bulding 348, DK 2800 Kgs. Lyngby, Denmark

**Abstract**—This paper focuses on statistical modeling of water vapor fluctuations for InSAR. The structure function and power spectral density approaches are reviewed, summarizing their assumptions and results. The linking equations between these modeling techniques are reported. A structure function model of zenith tropospheric propagation delay is then derived from a two-regime power spectral density function presented in literature. The novelty lies in the fact that a closed form expression is derived and a free model parameter is allowed, which may be tuned to available measurements or, in the absence of these, to atmospheric statistics. The latter approach is used to compare the derived model with previously published results.

**Keywords**- SAR interferometry; atmospheric propagation delay; statistical modelling.

## I. INTRODUCTION

Several InSAR applications exploit expressions for the auto-covariance function of atmospheric propagation delay. Examples are error prediction for height and displacement measurements obtained with a minimum number of interferograms [1, pg. 61], data selection process within multi-interferogram frameworks [2] and atmospheric error correction using GPS [3] or satellite imaging spectrometers [4], [5], combined with statistical interpolation techniques [6].

In the following, modeling of propagation delay due to temporal variations in the spatial distribution of tropospheric water vapor shall be considered. The effects of ionosphere and of changes in the vertical profile of tropospheric refractive index may not be neglected in general, although they shall not be discussed further in this work.

In order to exploit a wealth of modeling results obtained within the radio wave propagation [7]-[8], GPS [2], [3] and VLBI [9] communities, it is convenient to relate the sought auto-covariance to the zenith delay structure function, which is the quantity discussed in these studies. At the same time, the results of more recent and InSAR-specific researches, involving extensive comparisons with meteorological data, are stated in terms of power spectral density (PSD) of the interferometric phase artifacts [1], [10]-[12].

In this paper, the approach has been to derive a structure function model from an InSAR-based PSD expression [1], [11]. In doing so, also the physical insight and some techniques developed in spatial-domain modeling contexts [3], [8], [9]

have been exploited. This procedure has the benefit of producing a closed form and tunable model, based on InSAR observations, and readily related to the statistics useful for applications.

## II. STATISTICAL MODELLING APPROACHES

### A. Refractivity and delay structure functions

In several researches statistical modelling of water vapor fluctuations has been based upon the structure function of atmospheric refractivity (1). The latter is defined as  $N=10^6 \cdot (n-1)$ , where  $n$  is the atmospheric refractive index.

$$D_N(\vec{r}, \vec{R}) = E \left[ \left( N(\vec{r} + \vec{R}) - N(\vec{r}) \right)^2 \right] \quad (1)$$

In (1)  $\vec{r}$  and  $\vec{R}$  represent the 3-dimensional position and displacement vector respectively and the expected value is taken over all possible atmospheric states. The quantity of interest is wavefront delay, which results from an integration of  $N$  and is thus a two dimensional quantity. In the following the one-way zenith delay (or zenith excess path length) shall be indicated with  $\tau$  and its units shall be meters. In several independent studies, [8], [9], [1], the following two regime power law for  $D_\tau(R)$  has been observed and a third "saturation" regime is conjectured, based on physical constraints:

$$D_\tau(R) = \begin{cases} C_i^2 R^{5/3} & L_0 \ll R \ll L_1 \\ C_L^2 R^{2/3} & L_1 \ll R \ll L_2 \\ C_L^2 L_2^{2/3} & R \gg L_2 \end{cases} \quad (2)$$

In (2)  $R$  represents horizontal distance,  $L_0$  the inner scale of dissipation,  $L_1$  the outer scale of injection and  $L_2$  the saturation scale length. Finally  $C_i$  and  $C_L$  are the structure constants of the turbulence. Functional dependence on  $R$  requires the hypothesis of homogeneity (wide-sense stationarity) and isotropy (circular symmetry).

It is agreed among the above mentioned studies that the first regime corresponds to a three-dimensional Kolmogorov turbulence [7] and  $L_1$  should be in the order of a few kilometers.  $L_0$  is instead in the order of millimeters [8], and is therefore not relevant for current SAR interferometers. For the second regime, it has been observed in [8] that everything goes

J.P. Merryman Boncori was supported by a grant from the Geoinformation Ph.D. programme, University of Rome "Tor Vergata".

as if Kolmogorov's "2/3 law" describing isotropic turbulence, could be extended also to scales larger than the tropospheric thickness, provided turbulent motion is considered two-dimensional in character. This interpretation is also currently accepted by other authors [10] and implies proportionality between the delay and the refractivity structure functions through the square of the effective tropospheric height. This fact is relevant for the present discussion and shall be referred to in section IIIB. Finally, for even larger scales, in the order of several hundred kilometers, the structure function is bound to "saturate", otherwise it would represent an infinite variance of the long-term atmospheric disturbance [9]. Anyhow, as far as modeling is concerned, very different values have been proposed for  $L_1, L_2$ .

### B. Power spectral density of phase artifacts

A more recently proposed approach to the modeling of atmospheric artifacts in SAR interferometry is through the Power Spectral Density (PSD) of the phase variation associated to the excess path length. Considering two-way propagation along the zenith direction, the radar wave's phase  $\varphi$  is related to the one-way zenith delay  $\tau$  by:

$$\varphi = \frac{4\pi}{\lambda} \tau \quad (3)$$

The PSD of  $\varphi$  is found as the Fourier Transform of the autocovariance function

$$C_\varphi(\vec{r}, \vec{R}) = E\left[\left(\varphi(\vec{r}) - \mu_\varphi\right)\left(\varphi(\vec{r} + \vec{R}) - \mu_\varphi\right)\right] \quad (4)$$

In the above  $\vec{r}$  and  $\vec{R}$  represent the 2-dimensional position and displacement vector respectively whereas  $\mu_\varphi$  represents the mean of  $\varphi$  and will be assumed zero in the following. Assuming wide-sense stationarity and circular symmetry the autocovariance reduces to  $C_\varphi(R)$ , where  $R = |\vec{R}|$ . The one-sided PSD of  $\varphi$  may be computed through (5).

$$P_\varphi(f) = \begin{cases} 0 & f < 0 \\ 4 \int_0^{+\infty} C_\varphi(R) \cos(2\pi fR) dR & f \geq 0 \end{cases} \quad (5)$$

where  $f$  represents spatial frequency.

In order to link PSD and structure function models, it is first of all noted that (5) holds also between the zenith delay PSD and its autocovariance respectively, due to (3). Secondly, stationarity implies that the variance of the atmospheric delay,  $Var\{\tau\}$ , is assumed constant at every point in its two-dimensional space. Furthermore, under the hypotheses of stationarity and zero mean, the one-way zenith delay autocovariance function may be related to the corresponding structure function through (6).

$$C_\tau(R) = Var\{\tau\} - 0.5 D_\tau(R) \quad (6)$$

In [9] a notation convention is introduced, by which the symbol  $D_\tau(\infty)$  is used to represent the delay structure function

value at a distance at which delay observations are uncorrelated. From (6) it follows that  $D_\tau(\infty) = 2Var\{\tau\}$ .

The autocovariance,  $C_\varphi(R)$ , is found by taking the inverse Fourier transform of the two-sided PSD, which by using (6) and (3) leads to:

$$D_\tau(R) = \left(\frac{\lambda}{4\pi}\right)^2 \int_0^\infty 4 \sin^2(\pi fR) P_\varphi(f) df \quad (7)$$

see also [1, pg. 274].

Equations (5), (6), and (7) analytically relate PSD and second order statistic modelling. The convenience of PSD modelling lies in the fact that the disturbances on SAR phase caused by a variety of weather conditions, from thunderstorms to clear sky, were found to comply to a similar two-regime model [1]. Based on [11] and [1, pg. 146], the following closed form may be written:

$$P_\varphi(f) = \begin{cases} \left(hf_0\right) P_0 \left(\frac{f}{f_0}\right)^{-5/3} & \frac{1}{R_{max}} < f \leq \frac{1}{h} \\ P_0 \left(\frac{f}{f_0}\right)^{-8/3} & \frac{1}{h} < f \leq \frac{f_s}{2} \end{cases} \quad (8)$$

In the above  $h$  represents effective tropospheric height,  $f_0$  is an arbitrary spatial frequency greater than  $1/h$ ,  $P_0 = P_\varphi(f_0)$ ,  $R_{max}$  is the maximum distance between a pair of SAR image pixels and  $f_s$  the data sampling rate used in the derivation of (8). The validity of the former at low and high frequencies has been limited since compliance outside these scales has actually not been observed in SAR data. This is due to the limited size of SAR images for low frequencies and to the dominance of thermal noise for high ones. Namely, (8) was verified for  $R_{max} = 50$  km and  $f_s = (1/160)$  m<sup>-1</sup>. It is expected that as spatial frequency decreases (below one cycle in several hundred kilometers), the delays become uncorrelated and the PSD will tend to flatten. The behavior at high frequencies (above 1 cycle in tens of meters) is not of great concern due to the small amplitude of atmospheric disturbances compared to other noise sources.

## III. PROPOSED MODEL

### A. Derivation

The statistics of interest for the interferometric SAR applications mentioned in section I are the covariance  $Cov\{\delta_i, \delta_j\}$  and the variance  $Var\{\delta_i - \delta_j\}$ , where  $\delta_i$  represents the slant range atmospheric delay of the  $i$ -th interferogram pixel ( $\delta_i = (\lambda/4\pi)\Delta\varphi_i$ , where  $\Delta\varphi_i$  is interferometric phase). Assuming the atmospheric states at the interferometric pair acquisition times to be uncorrelated and described by the same one-way zenith delay structure function,  $D_\tau(R)$ , the sought quantities are

$$Cov\{\delta_i, \delta_j\} = m^2(\theta) (D_\tau(\infty) - D_\tau(R)) \quad (9)$$

$$Var\{\delta_i - \delta_j\} = 2m^2(\theta) D_\tau(R)$$

where  $\theta$  is the mean radar angle of incidence,  $m(\theta)=\cos^{-1}\theta$  and  $R$  the horizontal distance between pixels  $i$  and  $j$ .

A closed form for  $D_\tau(R)$  may be derived from the one-sided phase PSD in (8), using (7). For convenience in the mathematical derivation, the maximum distance between two image pixels,  $R_{max}$ , as well as the sampling frequency  $f_s$ , which appear in (8), will be set to infinity. The former assumption implies the spectrum will not flatten for low spatial frequencies, which in turn implies an infinite variance for the atmospheric phase disturbance. This unphysical assumption however will be corrected for in the spatial domain, following an approach proposed in [9]. The latter assumption instead is expected to have little impact on the derivations, due to the low power levels associated with increasing spatial frequencies in comparison with thermal noise. Inserting (8) into (7) yields the following, after a change of variables and reordering:

$$D_\tau(R) = P_0 C_0 \left[ C_1 I_1 \left( \frac{R}{h} \right) R^{2/3} + C_2 I_2 \left( \frac{R}{h} \right) R^{5/3} \right] \quad (10)$$

$$C_0 = \left( \frac{\lambda}{4\pi} \right)^2, \quad C_1 = 4f_0^{8/3} \pi^{2/3} h, \quad C_2 = 4f_0^{8/3} \pi^{5/3}$$

$$I_1 \left( \frac{R}{h} \right) = \int_0^{\pi R/h} u^{-5/3} \sin^2(u) du$$

$$I_2 \left( \frac{R}{h} \right) = \int_{\pi R/h}^{\infty} u^{-8/3} \sin^2(u) du$$

The computation of the above integrals may be done numerically, however a closed form is of practical interest and an accurate approximation is reported in (11).

$$I_1 \left( \frac{R}{h} \right) = \begin{cases} \frac{3}{4} u^{4/3} - \frac{1}{10} u^{10/3} & \frac{R}{h} \leq A_1 \\ C_3 - \frac{3}{4} u^{-2/3} & \frac{R}{h} > A_1 \end{cases} \quad (11)$$

$$I_2 \left( \frac{R}{h} \right) = \begin{cases} C_4 - 3u^{1/3} + \frac{1}{7} u^{7/3} & \frac{R}{h} \leq A_2 \\ \frac{3}{10} u^{-5/3} & \frac{R}{h} > A_2 \end{cases}$$

In (11)  $u=\pi R/h$  and the values of the constants are reported in Table 1. The accuracy of the closed form approximation is further discussed in section IV.

### B. Convergence at infinity

It has been pointed out in [9] that a power law structure function leads to an unphysical feature at infinity, since tropospheric delay should be uncorrelated for two infinitely distant points. Following the approach of [9], a multiplying factor is introduced to provide convergence of the structure function at infinity. The same factor used in [9] for the refractivity structure function is used here for the delay structure function, based on the proportionality of the two for  $R \gg h$  discussed in section IIA. Therefore the model can be modified, leading to (12).

$$D_\tau(R) = P_0 C_0 \left[ \frac{C_1 I_1 \left( \frac{R}{h} \right) R^{2/3}}{\left[ 1 + \left( \frac{R}{L} \right)^{2/3} \right]} + C_2 I_2 \left( \frac{R}{h} \right) R^{5/3} \right] \quad (12)$$

### C. Tuning of model parameters

In order to use the delay structure function model (12), parameters  $P_0$  and  $L$  must be computed. In the absence of any scene-specific information, published atmospheric delay statistics may be used. Assuming ergodicity and that the spatial structure of the turbulence is "frozen" and moves with a constant wind speed  $s$ , spatial and temporal statistics may be interchanged so that distance  $R$  corresponds to  $st$ , where  $t$  is the time variable. Measured delay variances over a time  $T$  and the model expressions (12) and (11) can then be used to setup two equations in the two unknowns  $P_0$  and  $L$  as follows [9]:

$$\lim_{R \rightarrow \infty} D_\tau(R) = 2 \cdot \text{Var}\{\tau\} \approx 2 \cdot \sigma_\tau^2(T) \Big|_{T=1\text{year}} \quad (13)$$

$$\frac{1}{T^2} \int_0^T (T-t) D_\tau(R) \Big|_{R=st} dt = \sigma_\tau^2(T) \Big|_{T=24\text{hr}} \quad (14)$$

Equation (13) enforces a finite long-term (long-distance) variance,  $\text{Var}\{\tau\}$ . Annual measurements may be used. Equation (14) enforces agreement with a second (short-term) variance measurement. Equations (13) and (14) can be solved iteratively, initializing  $L$  to the 3000 km value reported in [9] and using globally representative values for the long and short-term variances. Physically reasonable values for  $P_0$  are expected to range from 1 to 40 m, according to the observations of [1], whereas  $L$  should be between 800 and 3000 km according to [2] and [8].

Should a PSD measurement at a certain spatial frequency be available at an acquisition time, this would provide a value for  $P_0$  in (12) and  $L$  could be computed from (13).

## IV. COMPARISON WITH PREVIOUSLY PUBLISHED RESULTS

A closed form model was obtained tuning the free parameters ( $P_0, L$ ) in (12) to globally representative atmospheric statistics, using (13) and (14). The expressions reported in (11) were used. For comparison a model was also derived, with integrals  $I_1$  and  $I_2$  evaluated numerically. The model parameters  $h$  and  $s$  were in both cases set to 3 km [11] and 8 m/s [9] respectively. The procedure outlined in the previous section was used to compute  $P_0$  and  $L$ , using 1 cm and 2.4 cm as the measured daily and annual rms of atmospheric delay [9]. A list of all model parameters is reported in Table I. The reported  $P_0$  and  $L$  values are those of the closed form model, which differ only slightly from those computed for the numerical one.

A first comparison between the numerical and the closed form structure functions derived in this letter is plotted in Fig. 1. The relative error, due to the approximations used in deriving (11), amounts to less than 5 % and causes an error of less than 0.1% in the interferometric path length covariance.

The former was computed through (9). These error figures are negligible for applications, and in the following only the closed form model shall be considered.

TABLE I. STRUCTURE FUNCTION MODEL PARAMETERS.

Parameter	Value	Unit	Description
$P_0$	9.04	m	$P_\varphi(f_0)$
$f_0$	1	$\text{km}^{-1}$	arbitrary spatial frequency
$L$	2133	km	saturation scale length
$h$	3	km	tropospheric height
$s$	8	m/s	tropospheric wind speed
$A_1$	0.472	-	constant
$C_3$	1.4731	-	constant
$A_2$	0.466	-	constant
$C_4$	3.2177	-	constant

Parameter  $f_0$  was chosen arbitrarily, whereas  $P_0=P_\varphi(f_0)$  and  $L$  were computed solving (13) and (14), using 1 cm and 2.4 cm as the daily and annual rms of zenith atmospheric delay. Parameters  $h$  and  $s$  were assigned based on [11] and [9] respectively.

Secondly, the closed form structure function of this letter was compared to that of Treuhaft and Lanyi [9], plotted as a dashed line in Fig. 1 (left). The greatest relative difference is observed around  $R=h$ , and amounts to about 30% whereas the corresponding difference in interferometric path length covariance grows to 1.5 % over a 100 km distance. The observed differences are imputable to the piecewise approximation of the PSD in (8), used to derive this letter's model, as well as to the different value of  $h$  chosen (3 km in this work as opposed to 1 km in [9]).

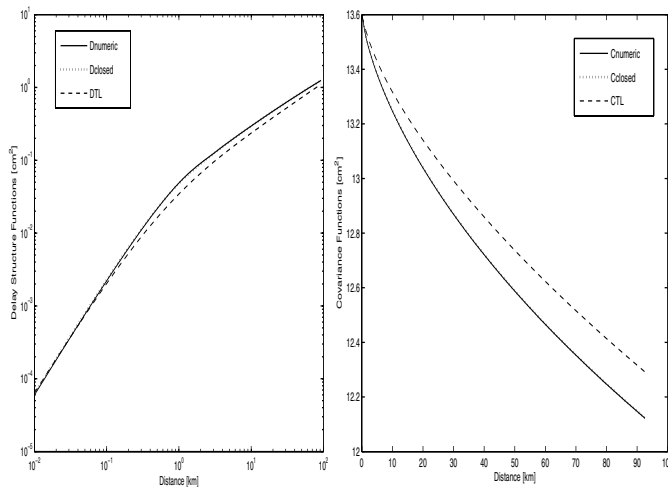


Figure 1. (left) Closed form and numeric delay structure functions derived in this study (continuous and dotted line respectively) compared to that of [9] (dashed line). (right) Corresponding interferogram path length covariances (9) assuming similar atmospheric state at the two acquisitions.

A third comparison was carried out in the spatial frequency domain. The phase PSD corresponding to (12) was computed using the values in Table I. The relative differences with (8), due to the denominator in (12), were found to be below 15% over typical SAR spatial scales. Considering the uncertainties in the scene dependant model parameters  $h$ ,  $s$  and  $P_0$ , it may be

assumed for all practical purposes that parameter  $P_0$  in (12) still represents the corresponding PSD at  $f=f_0$ . Furthermore, the  $P_0$  value derived in this letter (Table I) was found to be a median value compared to the values reported in [1], corresponding to a variety of weather conditions.

## V. CONCLUSIONS

A model for the second order statistics of the propagation delay associated with spatio-temporal refractivity fluctuations in the troposphere was derived. A closed form expression for the zenith delay structure function was obtained from a two-regime power spectral density function reported in literature [1],[11]. The underlying assumptions are wide-sense stationarity and circular symmetry of the considered process. The model contains four independent parameters, namely effective tropospheric height, effective wind speed, correlation distance and the power spectral density at a given spatial frequency. The latter may be computed exploiting acquisition specific information as well as "off the shelf" tropospheric delay statistics.

## REFERENCES

- [1] R.F. Hanssen, *Radar Interferometry: Data Interpretation and Error Analysis*, Kluwer Academic Publishers, Dordrecht, 2001.
- [2] T.R. Emardson, M. Simons and F.H. Webb (2003), "Neutral atmospheric delay in interferometric synthetic aperture radar applications: Statistical description and mitigation", *J. Geophys. Res.*, Vol. 108, No. B5.
- [3] S. Williams, Y. Bock, and P. Fang, "Integrated satellite interferometry: Tropospheric noise, GPS estimates and implications for interferometric synthetic aperture radar products", *J. Geophys. Res.*, Vol. 103, pp. 27,051–27,067, 1998.
- [4] Z. Li, J.-P. Muller, P. Cross, and E.J. Fielding, "Interferometric synthetic aperture radar (InSAR) atmospheric correction: GPS, Moderate Resolution Imaging Spectroradiometer (MODIS), and InSAR integration", *J. Geophys. Res.*, Vol. 110, No. B3, 2005.
- [5] Z. Li, E.J. Fielding, P. Cross, and J.-P. Muller, "Interferometric synthetic aperture radar atmospheric correction: MEdium Resolution Imaging Spectrometer and Advanced Synthetic Aperture Radar integration", *Geophys. Res. Lett.*, 33, 2006.
- [6] Z. Li, E.J. Fielding, P. Cross, and J.-P. Muller, "Interferometric synthetic aperture radar atmospheric correction: GPS topography-dependent turbulence model", *J. Geophys. Res.*, 111 (B2), 2006.
- [7] (cit. in [1]) V.I. Tatarski, 1961, *Wave Propagation in Turbulent Medium*, McGraw Hill Book Co., New York.
- [8] A.A. Stotskii, "Concerning the fluctuation characteristics of the earth's troposphere", *Radiophysics and Quantum Electronics*, Volume 16, Number 5 / May, 1973, Springer New York (translated from russian).
- [9] R. N. Treuhaft, and G. E. Lanyi, "The effect of the dynamic wet troposphere on radio interferometric measurements", *Radio Science*, Vol. 22, No. 2, pp. 251–265, 1987.
- [10] R. Hanssen, A. Ferretti, M. Bianchi, R. Grebenitsharsky, F. Kleijer, A. Elawar, "APS Estimation and Modeling for Radar Interferometry", in *Proc. Fringe 2005*, <http://earth.esa.int/fringe2005/proceedings/>.
- [11] R.F. Hanssen, D.N. Moiseev, and S. Businger, "Resolving the acquisition ambiguity for atmospheric monitoring in multi-pass radar interferometry", in *Proc. IGARSS'03*, Toulouse, France, 21-25 July 2003, (cdrom).
- [12] R.F. Hanssen, "Atmospheric heterogeneities in ERS tandem SAR interferometry", DEOS report, No 98.1, Delft, 1998.